ISSN: 2414-1895 DOI: 10.6919/ICJE.202110_7(10).0032

# Sliding Mechanism and Cause Analysis of Hanyuan Landslide in Sichuan Province

Chen Huang[1], Youyi Zhang[1]

[1]School of civil Engineering and architecture, Southwest University of Science and Technology, 59 Qinglong Road, Mianyang, Sichuan 621010, China.

## Abstract

**On August 21, 2020, Fuquan Town, Hanyuan County, Sichuan Province, landslide geological disasters, large rock landslides, landslides, destructive, causing huge losses to the local. This paper collects relevant data through field investigation. The movement and deformation mechanism and causes of Hanyuan landslide are analyzed, and the main results are as follows. 1. In recent years, the local surface of the landslide area has a certain tensile deformation, and the terrain changes greatly in the rear edge of the landslide and the steeper part of the middle and upper part of the landslide, forming a multi-stage dislocation platform. 2 The landslide is a traction landslide induced by rainfall. At present, it is in the stage of creep deformation. The failure mode is that the clay rock of Xigeda Formation is softened after soaking in groundwater, which leads to the decrease of shear strength and the formation of local bedding sliding at the edge of the scarp. 3. The landslide front is saturated, and the landslide is cut out from the shear outlet on the free face of the shear outlet. The transverse cracks at the trailing edge of the landslide continue to widen and deepen. 4. Under the action of continuous heavy rainfall, rainwater infiltrates into the sliding body and sliding surface, and sliding will occur. The landslide coverage directly slides out and accumulates in the valley, and the rare debris flow may occur.**

## Keywords

**Landslide Activities; Sliding Mechanism; Formation Mechanism; Stability Analysis.**

## 1. Introduction

The formation mechanism and stability evaluation of landslide have always been the research focus of geological disasters. The results are closely related to the experience and methods of researchers [1]. Field investigation of geological disasters is the primary link in the study of geological disaster activities [2]. Effective for later landslide movement analysis provides a scientific basis. Through field investigation, we can quickly find out the basic characteristics of the failure mechanism of the landslide and the formation position of the sliding surface (belt) [3]. Landslide activity is mainly affected by material, structure and environmental factors, among which environmental factors are the most active. Studies have shown that most landslides are triggered by heavy rainfall [4,5]. However, due to the complexity and uncertainty of landslide activities, it is impossible to form a recognized stability analysis standard [6,7].

Xu Qiang et al [8]. proposed that the slope in the landslide formation area produced tensile cracks after the earthquake, and then under the influence of multiple aftershocks, their own gravity and heavy rainfall, eventually led to slope instability and failure. Wen et al [9]. proposed that the occurrence of landslide disasters was caused by the interaction of multiple factors such as earthquakes, heavy rainfall and gravity. Xie et al [10]. studied the dynamic characteristics of landslide by the material point method.

ISSN: 2414-1895 DOI: 10.6919/ICJE.202110_7(10).0032

In this paper, Hanyuan landslide is taken as an example. On the basis of field investigation and engineering drilling, the deformation process and movement mode of landslide are analyzed in detail, the movement mechanism and causes of Hanyuan landslide are revealed, and the stability of landslide is analyzed, which provides a certain reference for the prevention and control of geological disasters.

## 2. Study area

The landslide in the study area is located in Fuquan Town, Hanyuan County, Sichuan Province, about 16 km from Hanyuan County and 9 km from Fuquan Town. The geographical coordinates are E:102°38', N:29°22'. The elevation of landslide area is 848m~1061m, and the relative elevation difference is about 213m. The original landform of the landslide is a platform ridge slope, and the slope direction is NW16°–NE28°. South side is flat narrow ridge, width 70m~100m, slope down the development of two secondary platform, platform between steep slope, slope 35~45°, stepped ridge, ridge height 1.5~4m. The ‘V’ shaped valley was developed on the west side, with the overall gully direction of NE15° and the maximum cutting depth of about 50 m (Figure 1).

Fig. 1 3D oblique photography model of landslide area

According to the meteorological data of Hanyuan County for many years, the average annual precipitation is 730.8mm, mainly concentrated in May-October, accounting for 81.2 % of the annual rainfall, the minimum is 11mm in January, the maximum is 169.7mm in July. According to the data of Fuquan Xiangming rainfall station around the landslide area, the maximum annual rainfall of 50 years is 1036 mm (2018), the maximum annual rainfall of 20 years is 1036 mm (2018), and the maximum annual rainfall of 10 years is 1036 mm (2018). The maximum daily rainfall is88.7mm (2020), the maximum hourly rainfall is42.9mm (2020), the maximum10minutes rainfall is11mm (query the statistical parameters of rainstorm in Sichuan Province atlas).

According to the monitoring data of the rainfall station provided by Hanyuan Meteorological Bureau, during the rainfall cycle before the landslide, the maximum cumulative rainfall of 11 days from August 10 to the landslide was 225.6 mm, and the maximum rainfall on August 17 was 82 mm.

The landslide area is located on the left bank of Shahe River, the first tributary of Dadu River, and now on the left bank of Hanyuan Lake (Pubugou Hydropower Station Reservoir Area). The Dadu River is the largest tributary of the Minjiang River, with a total length of 1070 km and a length of 75.6 km. The basin area is 2171.5 km$^2$, with an average decline of 3.31 ‰. The average annual flow is 1407 m$^3$/s. The Liusha River is the largest tributary of the Dadu River in Hanyuan County, with a total length of 107 km and a basin area of 1170.3km$^2$. The annual average flow is 22.9 m$^3$/s, the minimum flow is 1.0 m$^3$/s, and the annual runoff is 725 million m$^3$.

The landslide area is located in the junction and merger of the Qinghai-Tibet, Yunnan-Myanmar-Indonesia giant zi ' structure and the western Sichuan tectonic belt of the Neocathaysian system, and is affected by the southern end of the Longmenshan tectonic belt of the Cathaysian system. The geological structure is complex, and the folds and faults are developed. The main outcrops are Yuanbaiguowan Formation (Tb), Tertiary and Quaternary sediments (NQ), Longtan Formation-Emeishan basalt group (Pl-e) (Figure 2).

Volume 7 Issue 10, 2021
DOI: 10.6919/ICJE.202110_7(10).0032

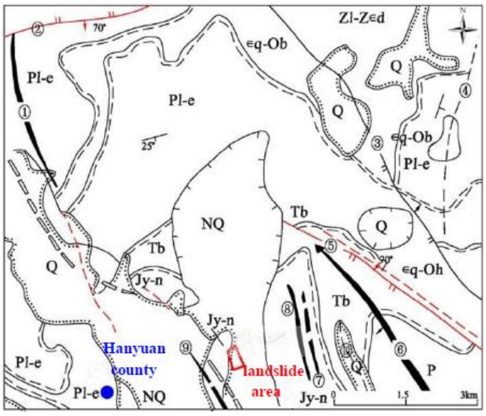

Fig. 2 Structural diagram of exploration area

## 3. Basic characteristics and hazards of landslide

The landslide is located in three groups of Zhonghai Village. The original terrain is as follows: the upper part is a gentle slope with a slope of about 15–30°; the middle part is a steep slope with a slope of about 6–70°; the lower part is a slope with a slope of about 20–35°. It is convenient to analyze the deformation mechanism of landslide and divide the landslide before sliding (H1-1, H1-2).

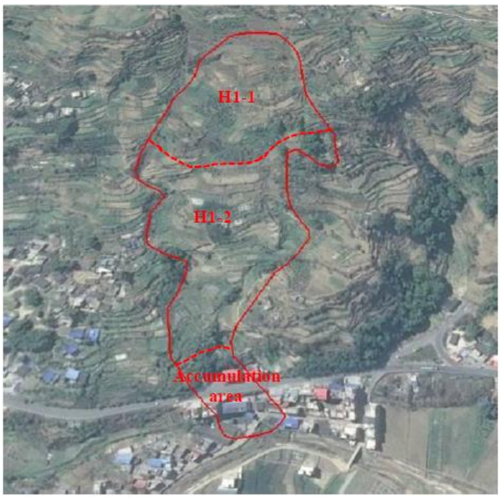

Fig. 3 Division before landslide slip

### 3.1 Evolution of landslide deformation and failure

#### 3.1.1 Landslide deformation stage

According to field survey visits, the H1-1 slide experienced three stages of deformation (Figure 4).

The first stage : the formation stage of the free surface. In 1985, tension cracks appeared in the middle and upper part of the landslide, landslide occurred in 1989, but the scale is relatively small. After the landslide, new scarps (free surface) appeared in the back of the landslide until May 12,2008, no new deformation cracks were found on the slope.

The second stage: early deformation -creep deformation intensified stage. After the 2008 Wenchuan earthquake, new tensile cracks appeared in the upper part of the scarp formed after the first stage. After the Lushan earthquake on April 20,2013, the cracks increased, enlarged, widened and the deformation intensified. The post-earthquake geological disaster survey in 2013 monitored the geological disaster points located at this point. With less aftershocks, the deformation of sliding body slowed down.

Volume 7 Issue 10, 2021
DOI: 10.6919/ICJE.202110_7(10).0032

The third stage: slip stage. From 8:00 on August 18 to 8:00 on August 20, 2020, the total rainfall in the landslide area reached 225.6 mm (70.6 mm from 8:00 on August 16 to 8:00 on August 17, and 76.2 mm from 8: 00 on August 17 to 8: 00 on August 18). On August 20, the deformation of tensile cracks in the rear area intensified and began to decline. At 3:50 a. m. on 21st, the sliding body slipped and repeatedly loaded to the top of H1-2 sliding body. The rest of the landslide material accumulated downward along the channel. The landslide material moved down rapidly along the channel and repeatedly scoured the loose material on both sides, causing the deformation of the loose material of H1-2 sliding body and moving downward together with the H1-1 sliding body material in a short period of time. It washed out along the front scarp. Some of the material accumulated in the current provincial road 345 and the outer residential area.

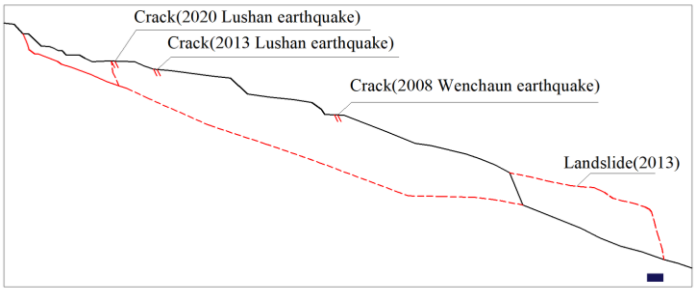


Fig. 4 Diagram of deformation evolution in landslide stage

### 3.1.2 Landslide factor

The Quaternary Xigeda strata are prone to collapse when encountering water. Under the action of external force and dynamic force, cracks appear at the back of the sliding body in each period of time step by step, which is beneficial to the infiltration of groundwater. Under the action of disintegration, the cracks are gradually deepened and widened, while the Xigeda strata are filled with clay rocks. Surface water infiltration softens clay rocks, reduces their physical and mechanical properties, and forms an unfavorable and stable layer. The front of the sliding body is a steep slope, which has the condition of free face. The two sides are gully. Under the action of channel cutting, the sliding body becomes an isolated rock mass. Under the action of gravity, the overall deformation and creep occur until a one-time slip occurs in a short time.


Fig. 5 Comparison of satellite photographs before and after landslide sliding

### 3.1.3 Landslide deformation mechanism

From the analysis of satellite images before and after the landslide, before the landslide sliding, the H1-1 landslide is a high and steep slope ( Figure 5), which is ladder-like. After the sliding, it is a flat slope, and the terrain changes greatly. The topography of H1-2 sliding body is similar before and after sliding (Fig. 5), and only changes after sliding and stacking in the central platform area.

From the historical analysis of landslide deformation, the deformation of H1-1 landslide has gone through the process of initial deformation, intensified deformation and progressive sliding. H1-2 landslide sign of H1-2 landslide in the three stages. Drilling reveals that no deep deformation is caused after sliding loading of H1-1 landslide (Xigeda formation), and only the deformation and sliding of loose material in the shallow surface layer are generated after the material on both sides of the channel is repeatedly scoured and eroded. Drilling reveals that the soil near the sliding surface has serious extrusion deformation traces (Figs. 6 and 7).

Fig. 6 Extrusion deformation of rock mass near sliding zone

Fig. 7 Extrusion deformation of soil near sliding zone

After investigation, Xigeda strata can be seen in the back wall of landslide cover, the inclination of strata is 90-130°, the dip angle is 10-13°, the inclination of regional strata is 45-60°, the dip angle is 30°, and the inclination of strata is quite different, which indicates that the original H1-1 landslide has produced displacement after deformation, so the slip occurs in the internal strata of Xigeda strata. Drilling shows that the dip angle of sliding surface of H1-1 landslide is 30°, which is consistent with the dip angle of rock stratum, so H1-1 landslide is bedding bedrock landslide.

To sum up, H1-1 sliding body generates sliding step by step, and the deformation mechanism of landslide is bedding traction bedrock landslide. H1-2 sliding body generates local shallow soil deformation and sliding at the moment of external force ( H1-1 sliding body loading and scouring ).

## 4. Basic characteristics of landslide

### 4.1 Current deformation characteristics of landslide

#### 4.1.1 Landslide subzone

Landslide zoning from the landslide deformation and failure characteristics combined with the status quo of landslide zoning (Figure 8), divided into sliding area landslide and residual body of two large areas, the residual body is divided into $I_1$, $I_2$, $I_3$, $II_1$, $II_2$ five sub-regions, sliding area for the early landslide sliding re-accumulation after the formation of new landslide, residual body according to the strength of the current deformation is divided into five sub-regions, including $I_1$, $I_2$, $I_3$ for a landslide residual body, $II_1$, $II_2$ for secondary landslide residual body.

#### 4.1.2 Status of landslide deformation

Landslide cover: after landslide sliding, it is re-stacked to form landslide cover, with slope direction of 20°, elevation of 875–1035 m, height difference of 160 m, and main sliding direction of 20°. The landslide structure is loose, the accumulation is disorderly, and the cracks on the slope are developed strongly (Fig.12). However, it is irregular. Due to the different sliding distances of the landslide in each block, many drum hill platforms, uplifts and depressions are formed on the landslide. The drum hill platform on the left side of the middle and upper part of the landslide is particularly obvious, and the water accumulation depression is formed on the right side of the middle part of the landslide. The back wall of the landslide forms up to 16 m staggered ridges (Figure 9) with a semi-circular distribution. The upper part of the ridge is a residual slope containing gravel clay silt, and the lower part is Xigeda siltstone, clay rock and fine sandstone. Clear scratches can be seen on both sides and posterior walls ( Figures 10, 11 ).

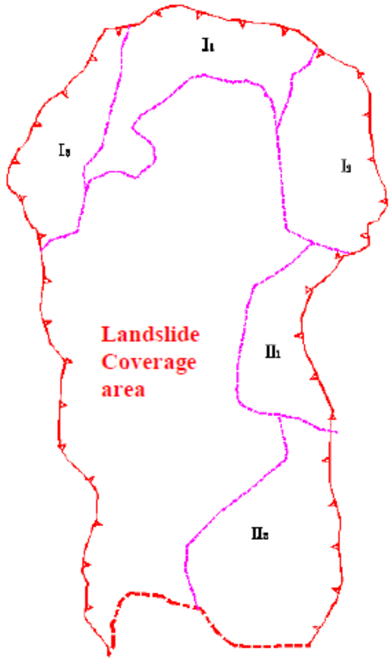


Fig. 8 Landslide zoning

Fig. 9 Backwall of landslide

Fig. 10 Right Sassafras mark of landslide

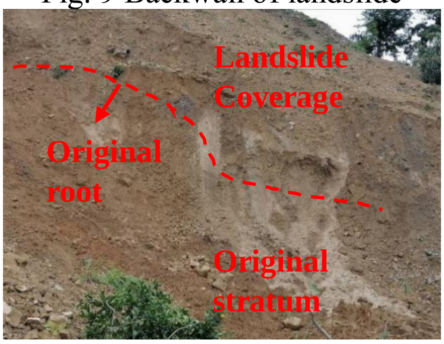


Fig. 11 $II_2$ Super-complex sliding body at the top of the region

Fig. 12 Cracks on landslide cover (new formation)

Most of the material in the upper surface layer of the original H1-2 landslide is accumulated after H1-1 sliding. There are many H1-1 landslide accumulation materials on the residual landslide ($II_2$ and $II_2$), and plant root layer can be seen between the layers. There are three plant roots in H1-ZK8 boreholes, and the depths are 10.5 m, 18.5 m and 20.3 m, respectively. It is proved that the area has undergone at least two sliding and stacking loads (0-10.5 m, 10.5-18.5 m and 20.3 m are residual soil

Volume 7 Issue 10, 2021
DOI: 10.6919/ICJE.202110_7(10).0032

on the original surface), which is also one of the evidence of landslide deformation and failure mode (H1-1 landslide sliding load causes shallow deformation and sliding of H1-2 landslide). The potential shear outlet of the landslide cover is located in the front edge of the landslide and the middle of the inner scarp of the provincial highway 345 (Figure 13). It can be seen that the stable rock stratum is exposed, and the occurrence is 50°∠16°, which is basically consistent with the occurrence of the regional rock stratum. At present, there is no swelling and large-scale collapse in the front edge, and only sporadic soil fall occurs locally. A gully is newly formed on the left side of the landslide cover from top to bottom (Figure 14). Long-term runoff is formed by the confluence of the upper slope of the landslide. The seepage flow in the landslide body is small, and the flow changes greatly with rainfall. The formation of the gully is easy to erode and cut the loose slope, which is beneficial to the infiltration of runoff into the landslide cover, and further soften the local soil, especially the loose material at the potential shear outlet, resulting in the collapse of the slope at the scarp, forming a structural layer that is unfavorable to the stability of the landslide cover, and has a great influence on the stability of the landslide.


Fig. 13 Front shear outlet of landslide

Fig. 14 Newly formed gullies on slides

### 4.2 Landslide boundary, morphology and scale characteristics

#### 4.2.1 Landslide cover

The trailing edge is bounded by the H1-1 landslide after sliding, the upper part of the left side is bounded by the gully extension 10-20 m, the lower part of the left side is bounded by the three groups of Gaoshanmiao landslide in Zhonghai village, and the right side is bounded by the groove after sliding. The potential shear outlet is located in the front of the landslide and the middle of the inner scarp of the provincial highway 345. The slope shape of the landslide cover is 'belt', the upper part is steep, the slope is about 40°, the middle and upper part is slow, the left side uplifts and bulges, the middle part is steep slope ( the original H1-1 front scarp slides and accumulates ), the slope is about 50°, the middle and lower part is slope, the slope is about 30°, the right side is depression, and the front edge is scarp (the original H1-2 shear outlet). The length of landslide cover is about 550m, the width is 90-220m, the average width is 135m, the area is $7.46\times10^4 m^2$, the thickness of landslide is 6-15m, the back is about 12m, the middle is about 5m, the front is about 8.5m, the average thickness is about 8m, the volume is about $63.4\times104m^3$.

#### 4.2.2 Residual body

The trailing edges of $I_1$ and $I_2$ are based on the last crack. According to the natural stable slope of sliding body 1:2 and the thickness of sliding body (10–15m), the extension of 10–30 m is the boundary. The two sides of $I_1$ are divided according to the deformation direction of sliding body. The right side of $I_2$ is bounded by the ridge watershed. The left side of $I_3$, $II_1$ and $II_2$ is bounded by the sliding steep slope. The right side is bounded by the leading edge by the ridge watershed. The residue size statistics are shown in table 1 ($II_1$, $II_2$ not deformed, not involved in statistics).

Volume 7 Issue 10, 2021
DOI: 10.6919/ICJE.202110_7(10).0032

Table 1. Statistical table of residue size

| Numbering | Longitudinal (m) | Average width (m) | Area ($\times10^4$m$^3$) | Thickness (m) | Average thickness (m) | Volume ($\times10^4$m$^3$) |
|---|---|---|---|---|---|---|
| $I_1$ | 239 | 57 | 1.37 | 6-10 | 8 | 10.9 |
| $I_2$ | 182 | 73.6 | 1.34 | 8-15 | 12 | 16.1 |
| $I_3$ | 205 | 49.7 | 1.02 | 6-15 | 11 | 11.2 |
| | | | Total | | | 38.2 |

In summary, landslide deformation is landslide cover, $I_1$, $I_2$, $I_3$ residual body. $II_1$, $II_2$ overall did not produce deformation, slope is relatively stable, in the calculation of landslide volume does not take its volume into account. The volume of landslide is about $125\times10^4$ m$^3$, which is a large landslide.

#### 4.2.3 Characteristics of sliding surface ( belt )

Landslide cover body: After sliding, there is no complete sliding zone in the landslide cover body at present. It is revealed by drilling and well exploration that the mirror feature of the sliding surface is obvious. The residual slope soil at the attachment of the picture is subjected to strong compression, deformation distortion, and local soil compaction. The sliding surface is a broken line with a slope of about 12~18°. The sliding surface is the contact surface between the Quaternary landslide accumulation layer and the Tertiary soil and rock, and the contact surface between the Quaternary landslide accumulation layer and the residual slope ( drilling reveals that there is no deep sliding surface in Xigeda ), and the buried depth is 5-16 m.

Residue: $I_1$, $I_2$, $I_3$ and $II_1$ sliding zones are clay rocks in Xigeda formation of Tertiary Oligocene. After clay rocks are saturated, the rock mass structure is destroyed, with soil properties (clay silt), soft plastic and slightly dense. $II_2$ is the local collapse of loose soil on the surface, and there is no unfavorable stable unified structural plane on the whole.

#### 4.2.4 Characteristics of slide bed

The sliding bed of landslide cover is Xigeda rock stratum of Tertiary Oligocene. According to drilling, the stratum is mainly composed of silty clay. Although the weak structural plane of soft clay rock is sandwiched in the stratum, the sliding surface is straight, continuous, and without faults. The local and overall surface is not empty on the undulating surface, and no deformation conditions are formed.

The residual body slide bed is the Tertiary Oligocene Xigeda strata. According to drilling, the strata are mainly composed of silt and clay. Although the weak structural plane of weak clay rock is sandwiched in the strata, there is no free surface in the deep weak structural plane and the upper material does not have sliding space.

#### 4.2.5 Landslide types

According to the material composition and structure form of landslide, $I_1$, $I_2$, $I_3$ belong to rock landslide, landslide cover is soil landslide. According to the thickness of landslide, it is middle landslide. In terms of motion form, it is a progressive bedding landslide. The cause is natural landslide. On the volume of landslide, it is a large landslide.

## 5. Influence factors and deformation failure mechanism of landslide

### 5.1 Landslide factor

According to the field geological mapping and drilling results, the main formation factors of this landslide are:

(1) Loose material basis. The material of landslide cover is accumulated after landslide sliding, and the thickness is 5–23 m. Although most of the residual body is rock mass, most of them have been deformed after early deformation, and the structure is basically destroyed, especially the material damage of rock mass $I_1$, $I_2$ and $I_3$.

(2) Unstable terrain conditions. At present, there is a new high and steep free surface at the leading edge of $I_1$, $I_2$ and $I_3$ residues, with a slope of 50–85°. After sliding, the slope gradient of the sliding body of the landslide covering body is 10–35°, and the slope of the leading edge is about 60–80°. It

also has the conditions of free surface, which makes favorable conditions for the formation of landslides.

(3) Infiltration of surface water. After landslide sliding, the terrain is lower than the slopes on both sides, forming grooves, which is conducive to the collection of surface water. At present, a gully is formed on the left side of the landslide, and long-term runoff is formed. In addition, the structure of the new accumulation landslide is loose, the content of gravel is large, and the infiltration rate of surface water is fast. Linear seepage can be seen at the front edge of the landslide cover. During continuous rainfall, the flow increases, and the collapse of the landslide soil is accompanied. The crack deformation of residual body at the trailing edge of landslide gradually becomes strong. Although emergency treatment measures (crack backfilling and film laying) are adopted, the infiltration of surface water can only be temporarily reduced. Linear seepage can be seen at the front edge of landslide ($I_1$, $I_2$, $I_3$), and at the steep slope. During rainfall, strand gushing water can be seen, accompanied by continuous collapse, and large-scale collapse can be seen in the front of $I_2$.

(4) Seismic action. The early landslide slip, seismic action is the incentive (cracks), landslide deformation has been formed after landslide slip, in the absence of earthquake and other external forces will also produce sustained deformation. Hanyuan area is located in the west end of Longmenshan fault. Although it is not a concentrated stress release area, it is close to the seismic wave and the influence area, and it is more frequent. Once the front sliding body slips, a new free appears. Under the action of seismic external force, new cracks appear in Xigeda stratum, and its deformation and failure mode is the same as that of the previous H1 -1.

Under the combined action of the above four factors, the landslide that has formed deformation and failure will accelerate the deformation, and it is more likely to deform again in the area where there is no obvious deformation in the rear. The scope of this landslide extends outward within the scope of deformation indications.

### 5.2 Deformation and failure mechanism of landslide

According to the drilling results, the landslide material of landslide cover is loose, and the sliding surface is the contact surface between the sliding material and the underlying Xigeda rock stratum. The sliding bed inclination is 50° and the dip angle is 30°. The overall slope is basically consistent with the terrain slope. The sliding surface is undulating and zigzag, and the surface water infiltration is strong. A stable seepage flow is formed on the sliding surface, and the stability of the landslide is poor. Due to the large free face of the leading edge, there are currently small-scale landslides that continue to fall and collapse during rainfall. Therefore, the landslide is pulled by the front, and the deformation of the rear soil will intensify. The landslide is a soil traction bedding landslide with broken line failure surface.

The cracks in the back of $I_1$, $I_2$ and $I_3$ slippery bodies run through the rock strata vertically, and deform and slide in the deep original weak structural plane, which is a deep bedrock bedding landslide. No deep deformation was found on the slope surface of $II_1$ and $II_2$ landslide, and the surface loose material collapsed locally at the scarp, resulting in the overall stability of the landslide.

## 6. Landslide stability evaluation

### 6.1 Calculation model and working condition

#### 6.1.1 Determination of calculation model

The landslide cover is formed by the accumulation of new landslide, and the sliding zone is not completely formed. Based on the above analysis of its failure mode, the sliding surface is a broken line, because there is the possibility of shearing out over the top of the landslide cover. According to the relevant requirements of Article 13.4 of '《Exploration specification of landslide prevention engineering》' (GB/T 32864-2016), the transfer coefficient method is used for the stability evaluation and thrust calculation of the landslide.

ISSN: 2414-1895 DOI: 10.6919/ICJE.202110_7(10).0032

The residual bodies of $I_1$, $I_2$ and $I_3$ had strong deformation, and the sliding surface had been formed. The sliding surface was calculated by using the sliding surface of comprehensive field and indoor analysis. The sliding surface was broken linear. The residual bodies of $II_1$ and $II_2$ were not deformed as a whole, and the sliding surface was not formed, and the sliding surface was linear.

#### 6.1.2 Determination of calculation condition

There are few buildings on the landslide, without considering the building load. The landslide is not submerged, regardless of the impact of flooding. The stable groundwater level was not measured during the slope exploration, so the hydrodynamic pressure of groundwater was not considered in the condition setting. The seismic intensity in this area is VII, and the seismic load should be considered. This area is characterized by concentrated rainfall and frequent rainstorm. The influence of rainstorm on slope loading and softening of sliding zone should be considered. Based on the above analysis and comprehensive consideration of the slope characteristics and various loads, the following conditions are selected to calculate and evaluate the landslide stability.

Table 2. Table of results of landslide stability calculation

| Rated section | Natural (k) | Natural + earthquake (k) | Cloudburst (k) |
|---|---|---|---|
| Before the landslide | 1.19 | 1.10 | 0.79 |
| After the landslide | 2.12 | 1.90 | 1.31 |

### 6.2 Landslide stability evaluation

This evaluation of the overall stability of the landslide is based on the evaluation criteria in 《Exploration specification of landslide prevention engineering》 (GB/T 32864 -2016): the stability coefficient $K < 1.0$ is an unstable state. $1.0 \leq K < 1.05$ is an unstable state. $1.05 \leq K < 1.15$ is the basic stable state. $K \geq 1.15$ is stable. Through the calculation and analysis of the main section of landslide, the following conclusions can be drawn :

Before landslide: In natural conditions, landslide stability coefficient is1.19, in a stable state. This is consistent with the actual situation that the landslide does not deform in the natural state. Under natural + seismic conditions, the landslide stability coefficient is 1.10, which is basically stable. It shows that the landslide has experienced '5.12 earthquake' and is still basically stable, which is consistent with the actual situation. Under the rainstorm condition, the landslide stability coefficient is 0.79, which is in the unstable sliding state. After the landslide sliding, the inner baffle of the lower fish pond is destroyed, and the fish in the fish pond is washed out on the lower highway. The landslide material is accumulated in the fish pond, which is consistent with the actual situation.

After landslide (currently): In natural conditions, landslide stability coefficient is 2.12, in a stable state. Under natural + seismic conditions, the landslide stability coefficient is 1.90, which is in a stable state. Under the heavy rain condition, the landslide stability coefficient is 1.31, which is in a stable state. In addition, due to the support effect of the masonry fortress outside the fishpond at the leading edge of the landslide, the landslide accumulation is in a stable state under three conditions, which is consistent with the actual situation and the calculation results are reliable.

## 7. Development trend of landslide

### 7.1 Forming a new landslide

From the above analysis, most of the material accumulated on the lower slope after the landslide H1-1 landslide slip, and the high material slips rapidly, scouring the loose deposits on both sides of the lower channel, causing the deformation and slip of the loose material of the H1-2 landslide. After the early landslide sliding, the accumulation body evolved into a new soil landslide, and formed a new free surface in the back wall. A large number of sliding bodies remained above the back wall. The formation of the new free surface provides potential energy conditions for the rear sliding body, and

ISSN: 2414-1895 DOI: 10.6919/ICJE.202110_7(10).0032

the deformation is intensified. According to its deformation characteristics, it is divided into three sliding blocks, and the possibility of re-sliding is great.

### 7.2 Stability of new landslide

According to the calculation, the landslide coverage, $I_1$, $I_2$ and $I_3$ are all in an unstable state under natural and saturated conditions. It can be seen that the shear outlets of each slide block produce sporadic or certain scale of drop and collapse. According to the monitoring data, the deformation on the slope increases cumulatively, and the landslide is in an unstable state.

### 7.3 Other

From the deformation mechanism analysis of H1-1 landslide, the occurrence of landslide is to have a large free surface, the second is the nature of rock mass itself is slippery stratum, the third is the occurrence of initial deformation under the action of external force ( the generation of cracks behind the landslide), the landslide range is determined according to the last deformation crack according to the 1:2 stable slope ratio extension of 20-30 m, but after the sliding of the rear sliding body, and the new free surface of the new city will affect its stability, so the factor should be taken into account in engineering protection and prevention.

After landslide sliding, a new accumulation body is formed, and a depression conducive to catchment is formed. The structure of accumulation material is loose, and surface confluence is easy to form water loss. During rainfall, it is expected that it will still be destroyed by slope debris flow and participate in debris flow activities in the future. During this survey, many slope debris flows occurred, but the rainfall is relatively small, and there is no large-scale debris flow outbreak. However, if concentrated continuous rainfall occurs, large-scale slope debris flow is likely to occur.

## 8. Conclusion

1) Although there is no sign of deformation outside the back of the landslide, a new surface will be formed once the landslide slips.

2) The influence of internal friction angle on landslide stability is greater than that of cohesion, that is, landslide stability is sensitive to internal friction angle.

3) Through investigation and study, it is believed that the main factor of slope instability is heavy rainfall. From the previous stability analysis, it can be seen that the shear strength of the sliding zone soil has a great influence on the stability of the landslide.

4) The water immersion of the trailing edge cracks and the enrichment and runoff of groundwater at the boundary between the base and the overlying strata generate hydrostatic pressure and seepage force, so that the sliding body undergoes traction sliding.

5) Loose accumulation bodies provide material basis for the formation of landslides. High and steep surface provides potential energy conditions for landslide formation. The action of water is the main inducing factor of landslide deformation and sliding.

## Acknowledgments

This research was funded by the National Key Research and Development Program of China (2018YFC1505401).

## Reference

[1] J.MA, M. Z. ZHANG, B.HAN, et al. Cloud platform construction for geological hazards' data from UAV survey [J]. The Chinese Journal of Geological Hazard and Control, Vol.30 (2019) No. 1,p. 100-105.

[2] C.Z.LIU. Basic problem on emergency disposition of abrupt heavy geological disaster[J]. Journal of Natural Disasters, (2006) No. 3, p. 24-30.

[3] N.P JU, J.J ZHAO, H.DENG, et al. Analysis of deformation mechanism of sliding to bending slope and study of deformation emergency control at Huangshan expressway [J]. Advances in Earth Science, 2008(5): 474-481.

[4] H.L.Wang. Analysis Method of Landslide Exploration Combined with Engineering Example [J]. Geotechnique, 2018, 33(4):194-198.

[5] W.G.Mu, H.C.Liu, D.L.Wang. Study on landslide control countermeasures of collapse accumulation close to buildings [J]. Geotechnical Engineering Technology, 2018, 32 (1):37-40,54.

[6] F.Q.Yuan. A Survey of Landslide Stability[J]. Water transport in China, 2009, 9(10):150-151.

[7] B.D.Xu. Qualitative Method and Technology of 'Contour Survey' for Diseases on Large and Medium Mountainous Slopes and Disease Control [M]. Beijing: China Railway Publishing House, 2016.

[8] Q.Xu, W.L.Li, X.J.Dong, et al. 2017. The Xinmocun landslide on June 24, 2017 in Maoxian, Sichuan: characteristics and failure mechanism [J]. Chinese Journal of Rock Mechanics and Engineering, 36(11): 2612-2628.

[9] M.S.Wun, H.Q.Chen, M.Z.Zhang, et al. 2017. Characteristics and formation mechanism analysis of the “6.24” catastrophic landslide of the June 24 of 2017, at Maoxian, Sichuan[J]. The Chinese Journal of Geological Hazard and Control, 28(03): 1-7.

[10] Y.F.Xie, X.P.Li, S.X ..Zhao, et al. 2018. MPM-based numerical analysis of the kinematic characteristics of Xinmo landslide in Maoxian County, Sichuan, China [J]. Mountain Research, 36(4): 589-597.